Indonesian Journal of Aerospace Vol. 23 No. 1 Juni 2025 : pp 45 – 56 (Zuhri)
DOI: 10.59981/ijoa.2025.9106
https://ejournal.brin.go.id/ijoa/

Flight Control Design for Rudder Failure Event on Cessna 172 Aircraft

Muhammad Rizki Zuhri

Department of Mechanical Engineering, Politeknik Negeri Bandung, Indonesia
e-mail: muhammad.rizki@polban.ac.id.

Received: 04-01-25 Accepted: 26-09-2025 Published: 05-10-2025

Abstract

The Cessna 172, a widely used small commercial aircraft, is renowned for its stability in both longitudinal and lateral-directional dimensions. Despite its intrinsic stability, a robust control system is essential to mitigate potential failures, such as rudder malfunctions. This study developed and simulated a control system for the Cessna 172 under rudder failure conditions, relying solely on aileron input for heading control. Using a linear state-space approach implemented in Matlab/Simulink, the control system incorporated yaw damping, roll damping, and heading hold for stability and waypoint tracking. Initial simulations showed that the controller could guide the aircraft to the destination waypoint but exhibited significant deviations of up to 20% under constant rudder inputs. Controller modification to the PID controller significantly improved performance, reducing deviations to a maximum of only 0.1% for ±5° rudder input. These results demonstrate the effectiveness of the proposed control system in compensating for rudder failure, though slight oscillations observed at the start of the trajectory suggest the need for further refinement. This research underscores the potential for adaptive and unconventional control methods to enhance safety and reliability in small aircraft operations.

Keywords: *Cessna 172; rudder failure; flight control; waypoint following.*

Nomenclature

β	:	Sideslip Angle	V	:	Aircraft's Velocity	ψ	:	Heading Angle
φ	:	Roll Angle	b	:	Aircraft's Wingspan	g	:	The Earth's gravitational constant
p	:	Roll Rate	δ_a	:	Aileron Input	l_{δ_a}	:	δ_a-to-p State-Space Component
r	:	Yaw Rate	δ_r	:	Rudder Input	l_{δ_r}	:	δ_r-to-p State-Space Component
y_β	:	β-to-β State-Space Component	y_{δ_a}	:	δ_a-to-β State-Space Component	n_{δ_a}	:	δ_a-to-r State-Space Component
y_φ	:	φ-to-β State-Space Component	y_{δ_r}	:	δ_r-to-β State-Space Component	n_{δ_r}	:	δ_r-to-r State-Space Component
y_p	:	p-to-β State-Space Component	l_β	:	β-to-p State-Space Component	n_β	:	β-to-r State-Space Component
y_r	:	r-to-β State-Space Component	l_p	:	p-to-p State-Space Component	n_p	:	p-to-r State-Space Component
			l_r	:	r-to-p State-Space Component	n_r	:	r-to-r State-Space Component

1. Introduction

Stability and controllability are essential attributes of an aircraft. An aircraft is considered stable if it can develop a restoring force or moment to bring it back to its original equilibrium condition. Meanwhile, controllability of an aircraft concerns whether the states of the aircraft's dynamics are affected by the control input (Nelson, 1998). These attributes are critical for all types of aircraft, from commercial jets to small planes, ensuring they can complete their missions safely. Stability and controllability also reduce pilot workload, thereby minimizing the risk of accidents.

In the context of time, two types of stability must be considered during aircraft design: static and dynamic stability. An aircraft exhibits static stability when the forces and moments that arise after a disturbance tend to restore it to its original state (Adiputra & Rohmanto, 2022). Dynamic stability, on the other hand, refers to the aircraft's ability to return to its initial equilibrium state over time, taking into account the magnitude and nature of oscillations (Jessica Davis, 2023). Both types of stability must be analyzed in the longitudinal and lateral-directional dimensions to declare an aircraft stable.

The Cessna 172 aircraft is one of the most popular small commercial aircraft in the world of aviation. Its widespread popularity is due to its simple, reliable, and safe design. In fact, the Cessna 172 is the most widely produced aircraft of all time (see Figure 1-1) (Niall McCarthy, 2021). The Cessna 172 is an American-made four-seater aircraft equipped with a single engine and a high-wing configuration. This aircraft is used for various aviation purposes, from flight training to a private aircraft.

The Cessna 172 was designed as a commercial aircraft that is stable in both the longitudinal and lateral-directional dimensions. Several studies have shown that the Cessna 172 is statically stable, as indicated by its derivative coefficient values, which meet the static stability requirements (Fadhilah, 2023; Kasnakoğlu, 2016; Vadivelu et al., 2020), as well as confirmed by flight test results (Marek M. Cel, 2019). Among them is the value of the derivative coefficient of the pitch moment to the angle of attack, which is negative ($C_{m_\alpha} < 0 C_{m_\alpha} < 0$), the value of the derivative coefficient of the roll moment to the angle of side slip is negative ($C_{l_\beta} < 0 C_{l_\beta} < 0$), and the value of the derivative coefficient of the yaw moment to the angle side slip is positive ($C_{n_\beta} < 0 C_{n_\beta} < 0$). Furthermore, the Cessna 172 aircraft control system also ensures that the aircraft is dynamically stable, so that the aircraft will return to an equilibrium state in a short time (Akyürek et al., 2016; Cessna Aircraft Company, 1998).

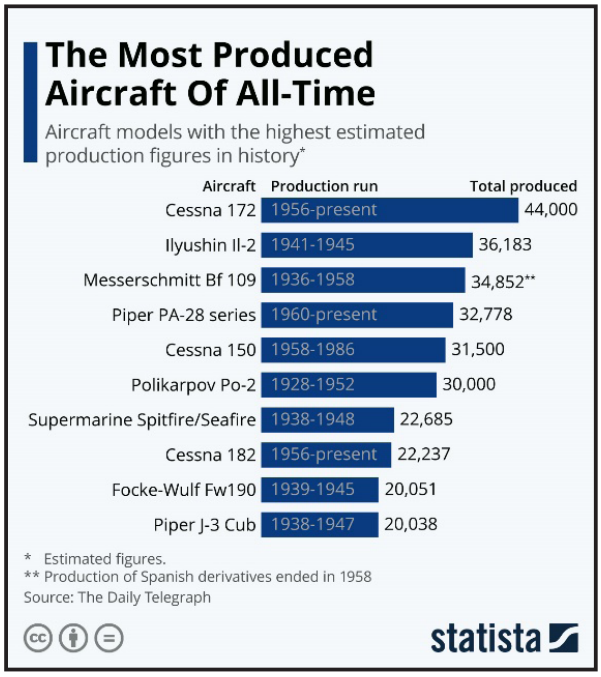

Figure 1: Sales Statistics of Various Aircraft Throughout History.

Even though the Cessna aircraft is intrinsically stable, the aircraft's control system must be designed to be tolerant of control failure, should it occur at any time. One failure that happens quite often is the failure of the aircraft's rudder. Failure of the rudder will make the aircraft unable to be controlled in its directional plane, leading to a situation where yaw movement is impossible. This imposes dangerous risks to the aircraft since it will lead to the aircraft's uncontrolled heading direction. In mid-1987, it was recorded that a Cessna 172 aircraft had an accident during landing due to the aircraft losing directional control (National Transportation Safety Board, 1987). Then, in 2005, a private Cessna 172 plane was forced to make an emergency landing shortly after landing due to the rudder not functioning properly (National Transportation Safety Board, 2005). In 2020, another Cessna 172 aircraft hit the ground after falling because of a rudder anomaly that caused the pilot to lose directional control (National Transportation Safety Board, 2020).

Research into improving flight controls for the Cessna 172 has yielded various approaches. Vadivelu et al applied non-conventional control in the form of changing the tail length to control the Cessna 172 aircraft in the longitudinal dimension (Vadivelu et al., 2020). Malik also developed a longitudinal dimension control system on the Cessna 172 aircraft by combining LQR and Fuzzy-PID-based control (A. Al-Isawi et al., 2020). However, these studies primarily focus on longitudinal stability. Prach developed a control system based on SDC (state-dependent coefficient), which is able to guide the aircraft for landing (Prach et al., 2019) and maintain the aircraft's attitude stable under wind disturbances in the form of turbulence to front and side winds (Prach, 2022). Despite these advances, Prach's work did not address control failures.

Given the frequency of rudder failures and the need for robust control systems, further research is necessary. This study addresses this gap by developing a control system for the Cessna 172 capable of compensating for rudder failure. Simulations are conducted in Matlab/Simulink using a linear state-space approach, focusing on lateral-directional dynamics. The system stabilizes the aircraft and guides it to a designated waypoint using aileron control in the absence of a functional rudder.

2. Methodology

This research implemented a numerical simulation of Cessna 172 lateral-directional stability. The derivative coefficients data for the Cessna 172 aircraft were obtained from Kasnakoğlu (Kasnakoğlu, 2016). The simulation was built in MATLAB/Simulink with a linear state-space approach. The dynamics of the aircraft in lateral-directional motion in the stability frame of reference are represented by the matrix expressions in Eq. 2-1 and 2-2 (Etkin & Reid, 1995; Nelson, 1998). Linearization is applicable to a specific trim condition. In this research, the aircraft was trimmed at a cruising speed of 65 m/s.

$$\dot{\bar{x}} = A\bar{x} + B\bar{u} \tag{1}$$

$$\begin{bmatrix} \dot{\beta} \\ \dot{\varphi} \\ \dot{\hat{p}} \\ \dot{\hat{r}} \end{bmatrix} = \begin{bmatrix} y_\beta & y_\varphi & y_p & y_r \\ 0 & 0 & \frac{2V}{b} & 0 \\ l_\beta & 0 & l_p & l_r \\ n_\beta & 0 & n_p & n_r \end{bmatrix} \begin{bmatrix} \beta \\ \varphi \\ \hat{p} \\ \hat{r} \end{bmatrix} + \begin{bmatrix} y_{\delta_a} & y_{\delta_r} \\ 0 & 0 \\ l_{\delta_a} & l_{\delta_r} \\ n_{\delta_a} & n_{\delta_r} \end{bmatrix} \begin{bmatrix} \delta_a \\ \delta_r \end{bmatrix} \tag{2}$$

However, since this research investigated a case of rudder failure, the rudder input was set to zero. Therefore, the pilot would be unable to control the aircraft's heading via rudder input. Alternatively, the pilot shall control the heading of the aircraft by using aileron input, utilizing the relation between turn rate and roll angle (Sadraey, 2020):

$$\dot{\psi} = \frac{g \tan(\varphi)}{V} \tag{3}$$

Assuming a small angle, $\tan(\varphi) \approx \varphi \tan(\varphi) \approx \varphi$ and implementing the Laplace transform, the following roll-to-turn transfer function is obtained:

$$\frac{\psi}{\varphi} = \frac{g}{sV} \tag{4}$$

The Simulink block for this research is represented in Figure 2-1. The model implemented a cascade control approach. The outermost loop served as the heading control for the aircraft, the second outer loop was the aircraft's roll damper, and the innermost loop became the yaw damper for the aircraft. These controls ensured stability of the aircraft in lateral-directional dimensions.

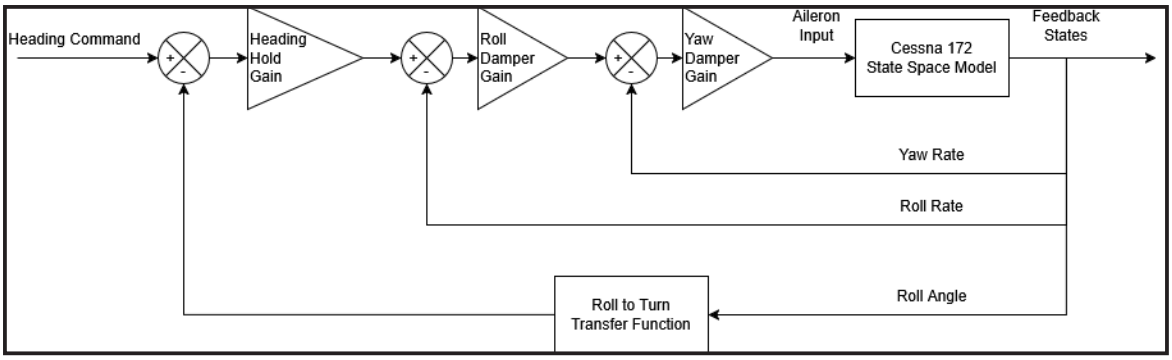

Figure 2: Simulink Block Model.

The aim is to determine the control gains that are capable of making the aircraft achieve the desired heading angle using aileron input, while also ensuring that the aircraft is stable by using the roll damper and the yaw damper. The control gains were chosen by investigating the transfer function for each loop, represented by its root locus diagram. The innermost control gain, yaw damper gain, was determined first, while the roll damper gain and heading hold gain were selected afterwards.

The heading command was evaluated by using a method proposed by (Fajar & Arifianto, 2018) (See Figure 2). The value of cross-track error (ε) is:

$$\varepsilon = R\sin(\psi_p - \psi_{ref}) \tag{5}$$

while ε is the cross-track error, i.e., the distance of the aircraft trajectory deviation to the desired trajectory, R is the distance between the previous waypoint to the aircraft position, ψ_p is the angle between R and the north direction, ψ_{ref} is the angle between the north direction to the line connecting the previous and current waypoints. The heading command was calculated as follows:

if $|\varepsilon| > \delta$, then

$$\psi_c = \psi_{ref} - sign(\varepsilon)\frac{\pi}{2} \tag{6}$$

if $|\varepsilon| \leq \delta$, then

$$\psi_c = \psi_{ref} - \frac{\varepsilon}{\delta}\frac{\pi}{2} \tag{7}$$

Where δ is the reference distance for the aircraft to turn, that is varied to obtain the desired trajectory, and ψ_c is heading the command for the aircraft.

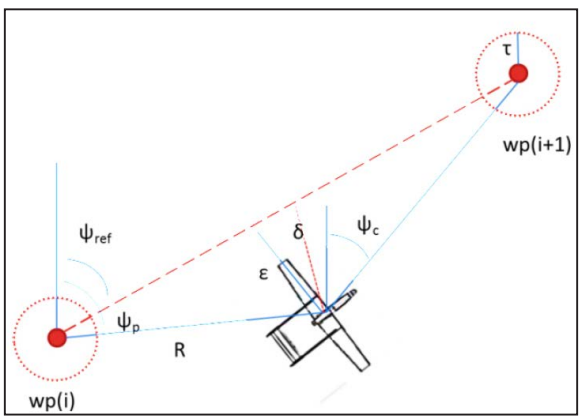

Figure 3: Aircraft Motion Towards Waypoints.

The position of the aircraft with respect to the local horizon frame of reference (North-East-Down, NED) is calculated by evaluating the aircraft's heading angle as follows:

$$x = \int_{t_0}^{t} V \sin \psi_p \, dt \tag{8}$$

$$y = \int_{t_0}^{t} V \cos \psi_p \, dt \tag{9}$$

where x and y are the aircraft's position in the NED reference frame, and $V$is the cruising speed of the aircraft.

3. Result and Analysis

3.1. Yaw Damper

Feedback gain for the yaw damper was determined using a root locus diagram. The input for the feedback gain is the yaw rate (r). The transfer function is represented in eq (1). The output of the feedback gain is the aileron input for the aircraft state-space. Figure. displays the root locus diagram for this system. The poles are all located on the left side of the real axis of the root locus diagram, indicating that all lateral-directional flight modes (Dutch roll, roll subsidence, and spiral) of the Cessna 172 aircraft are stable.

$$H_{yd}(s) = \frac{-6.273s^2 - 40.708s + 8.333}{s^4 + 10.785s^3 + 19.082s^2 + 84.773s + 0.943} \tag{10}$$

The gain evaluated was approximately 9, as it provides a good damping ratio while minimizing overshoot. Figure. 5 presents the comparison of the aircraft's response subjected to impulse input given various gain values. A gain value of 9 demonstrates better settling time, despite a slightly larger overshoot, compared to gain values of 7 and 11. Consequently, a gain of 9 was selected for the yaw damper.

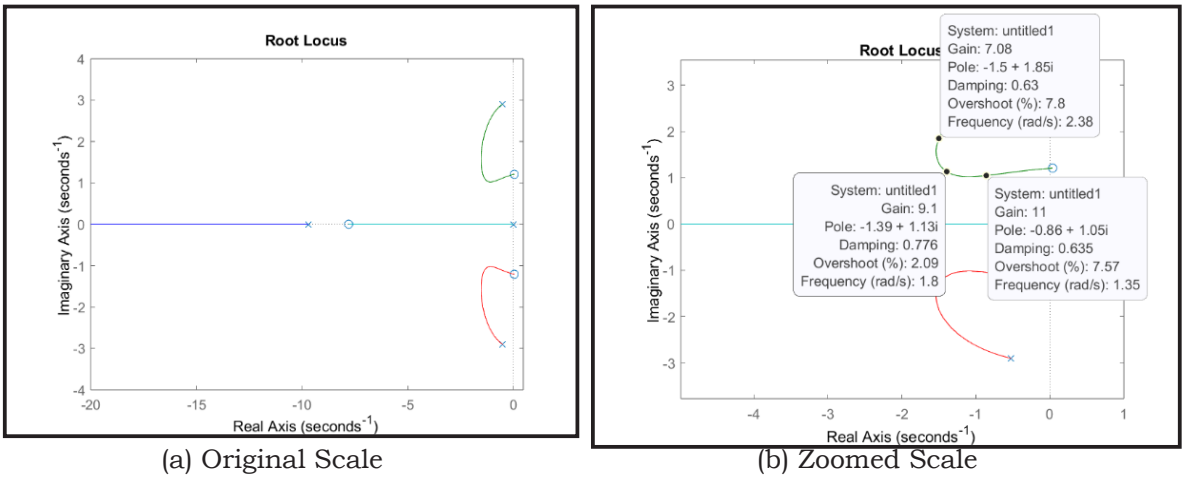

(a) Original Scale (b) Zoomed Scale

Figure 4: Root Locus Diagram for Yaw Damper System

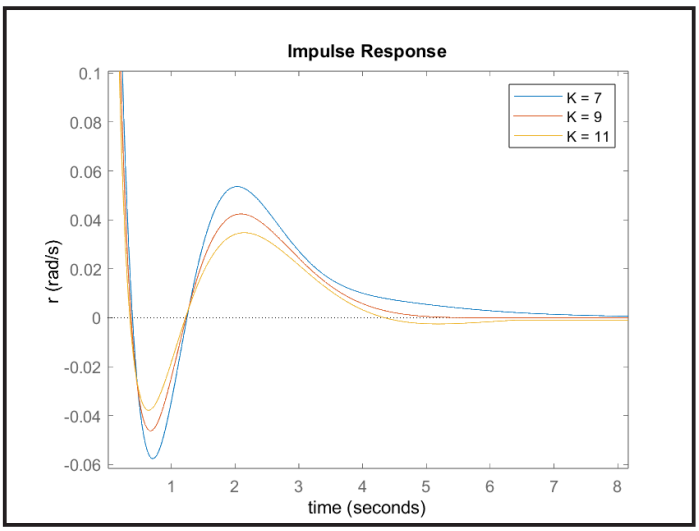

Figure 5: Yaw Rate Response for Different Gain

3.2. Roll Damper

For the root locus diagram analysis, the input for the feedback gain is the roll rate (*pp*), while the output is the aileron input. The plant is the aircraft state-space model equipped with the previously designed yaw damper. Eq (2) represents the transfer function for this system. Figure. 6 represents the root locus diagram for this system. All flight modes of the system, including dutch-roll, roll subsidence, spiral, and yaw damper control, are stable, as indicated by the poles located on the left side of the root locus diagram.

$$H_{ra}(s) = \frac{3.663s^3 + 5.118s^2 + 39.911s}{s^4 + 15.516s^3 + 55.649s^2 + 89.046s + 54.726} \quad (11)$$

The gain to be evaluated for roll damper control was approximately 0.05 because of its near-critical damping ratio and small overshooting. Figure. 6 illustrates the response of the aircraft's response to an impulse disturbance for different gain values. The gain value of 0.05 shows the largest overshoot compared to the other values. However, the gain values of 0.5 and 1 exhibit significantly longer settling time than that of the 0.05 gain value. Hence, a 0.05 gain value was selected for this system.

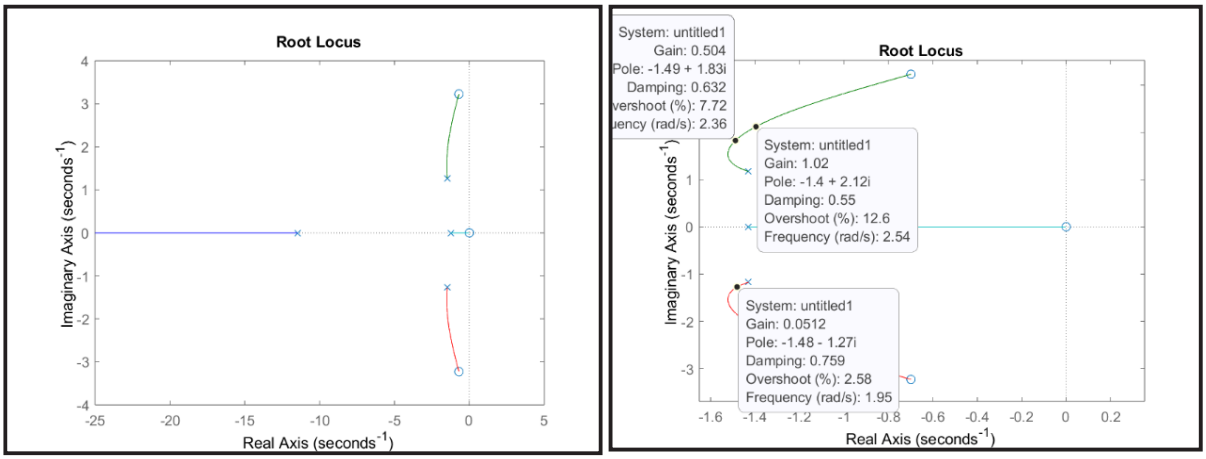

(a) Original Scale (b) Zoomed Scale

Figure 6: Root Locus Diagram for Roll Damper System

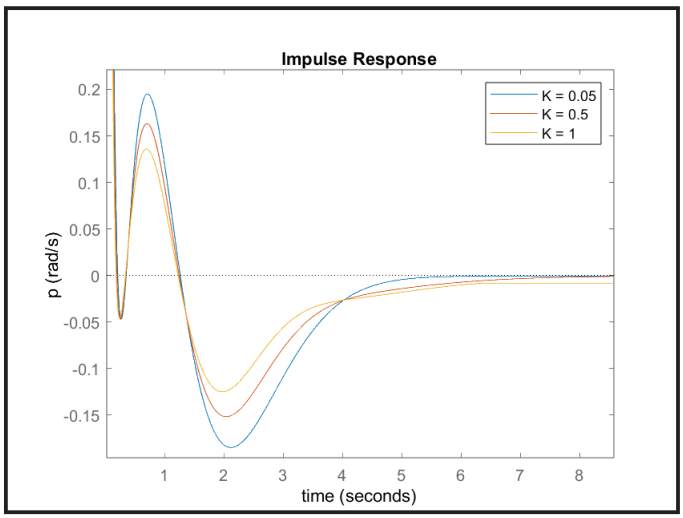

Figure 7: Roll Rate Response for Different Gain

3.3. Heading Hold

For the heading hold system, the input for the feedback gain is heading angle (ψ), while the output of the feedback gain is the aileron input. The plant is the aircraft state-space model equipped with the yaw damper and roll damper that have been designed. Figure. 8 shows the root locus diagram generated for this system. Eq (3) displays the transfer function used. Unlike the yaw damper and roll damper system, which have all stable poles, this system has two poles that eventually go to the unstable region, to the right side of the real axis. From Figure 3-5(b), it can be observed that the system becomes unstable when the gain value is approximately 1.44. Therefore, the gain selected must be below this threshold.

$$H_{hh}(s) = \frac{428.076s^2 + 598.135s + 4664.5}{65s^5 + 1020.4s^4 + 3633.8s^3 + 5917.7s^2 + 3557.3s} \quad (12)$$

The gain chosen for heading hold control was around 0.344 due to its favorable damping ratio and overshoot characteristics. Figure. 9 represents how the aircraft responded when an impulse disturbance is given for several gain values. A gain value of 0.15 resulted in a significant overshoot in the aircraft's heading response. While a gain value of 0.5 led to a reduced overshoot, the response was excessively oscillatory, resulting in a larger settling time. A gain value of 0.35 produced both minimal overshoot and a less oscillatory response. Thus, for the heading hold system, a gain value of 0.35 was selected.

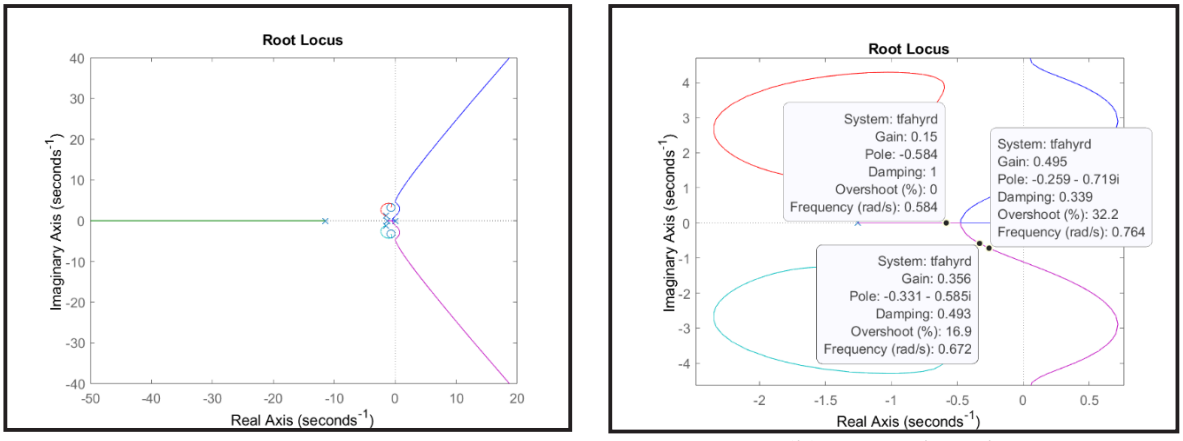

(a) Original Scale (b) Zoomed Scale

Figure 8: Root Locus Diagram for Heading Hold System

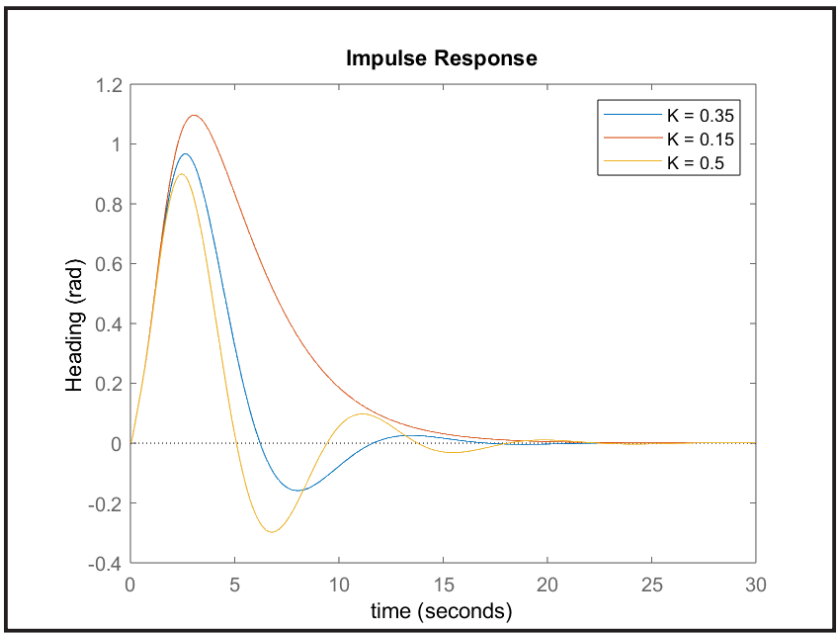

Figure 9: Heading Response for Different Gain

3.4. Waypoint Following

By the previous section, the controller had been designed by selecting a combination of gain values, as shown in Table 1. To evaluate the performance of the controller, a simulation of the aircraft following a waypoint under rudder failure was performed. As part of the simulation, fixed rudder inputs, representing the malfunctioning rudder, were included as a variation.

Table 1: Controller Gain Values

Controller	Gain Value
Yaw Damper	9
Roll Damper	0.05
Heading Hold	0.35

The simulation results are depicted in Figure 10. For zero rudder input, the designed controller successfully guided the aircraft to reach the destination waypoint starting from the origin. However, when the aircraft experienced a constant rudder input, the controller failed to guide the aircraft close to the target waypoint. A steady-state error appeared for the constant rudder input simulation. The deviation was approximately 250 m (12.5%) for ±3° rudder input and around 400 m (20%) for ±5° rudder input. These results indicate that the designed controller could not adequately compensate for a rudder failure event. To eliminate the steady-state error, integral and derivative gains were added to the controller, effectively transforming it into a PID controller. The integral and derivative gains were tuned using the PID tuner available in the Simulink PID Controller block, while the proportional gain was retained as specified in Table 3-1. The finalized gain values for the modified PID controller are summarized in Table 3-2.

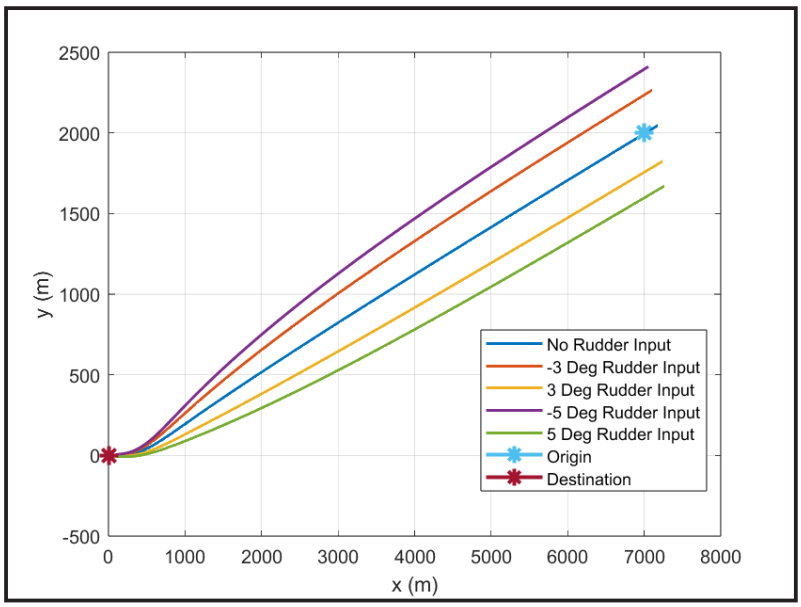

Figure 10: Aircraft Trajectory for Waypoint Following

Table 2: Controller Modified Gain Values

Controller	Kp	Ki	Kd	N
Yaw Damper	9	0.008	0.3	3
Roll Damper	0.05	0.008	0.5	3
Heading Hold	0.35	0.008	0.1	3

Figure 11 presents the simulation results for the aircraft's trajectory under rudder failure conditions with the modified controller. The controller successfully guided the aircraft to its destination across all simulation scenarios, exhibiting only minimal deviations. The largest deviation was observed in the simulation with a ±5° constant rudder input, resulting in a lateral error of just 2 meters (0.1%). These results highlight the significant improvement in trajectory tracking performance achieved by implementing a PID controller, as opposed to a proportional-only controller. However, this enhanced waypoint-following accuracy came with a trade-off: the aircraft experienced minor oscillations at the beginning of the trajectory as it approached the target.

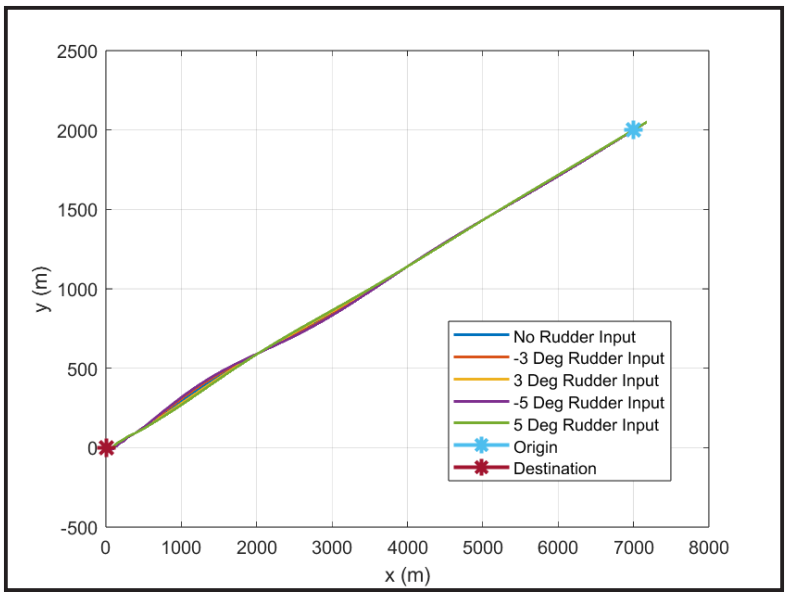

Figure 11: Aircraft Trajectory for Waypoint Following for Modified Gains

4. Conclusions

The controller for the Cessna 172 aircraft under the rudder failure event had been successfully designed. The controller included the yaw damper and roll damper for aircraft lateral-directional stability, as well as the heading hold, in order to achieve a specified targeted waypoint. The final design, which included a modification of the controller, successfully guided the aircraft to the destination, with minimal deviations for the simulations under constant rudder input.

There is still room for improvement for the proposed controller. The aircraft response indicated a slight oscillation at the beginning of the simulation, which is unfavorable. Unconventional controllers, such as Fuzzy Logic Controller, Sliding-Mode Control, etc., might be needed to eliminate this phenomenon. Moreover, an adaptive controller could also be employed since it has the ability to adapt to various cases of rudder malfunction.

Acknowledgements

The authors would like to thank the Department of Mechanical Engineering, Polban, for the support on this research.

References

A. Al-Isawi, M. M., Attiya, A. J., & ADOGHE, J. O. (2020). UAV Control Based on Dual LQR and Fuzzy-PID Controller. *Al-Khwarizmi Engineering Journal*, *16*(3), 43–53. https://doi.org/10.22153/kej.2020.08.001

Adiputra, B. D., & Rohmanto, A. (2022). PUNA Aircraft Static Stability Simulation Using XFLR5Software. *Compiler*, *11*(2). https://doi.org/10.28989/compiler.v11i2.1364

Akyürek, Ş., Özden, G. S., Atlas, E., Kasnakoğlu, C., & Kaynak, Ü. (2016). Design of a flight stabilizer system and automatic control using HIL test platform. *International Journal of Mechanical Engineering and Robotics Research*, *5*(1). https://doi.org/10.18178/ijmerr.5.1.77-81

Cessna Aircraft Company. (1998). *Cessna Model 172S - Information Manual*. Cessna.

Etkin, B., & Reid, L. D. (1995). Dynamics of Flight: Stability and Control (3rd Edition). *Wiley*.

Fadhilah, M. (2023). Analisis Kestabilan Statik Pada Konsep Uav Purwarupa Light Aircraft Dengan Konfigurasi Sayap Morphing Menggunakan Perangkat Lunak XFLR5. *JTT (Jurnal Teknologi Terpadu)*, *11*(1). https://doi.org/10.32487/jtt.v11i1.1636

Fajar, M., & Arifianto, O. (2018). PERANCANGAN AUTOPILOT LATERAL-DIREKSIONAL PESAWAT NIRAWAK LSU-05 (THE DESIGN OF THE LATERAL-DIRECTIONAL AUTOPILOT FOR THE LSU-05 UNMANNED AERIAL VEHICLE). *Jurnal Teknologi Dirgantara*, *15*(2). https://doi.org/10.30536/j.jtd.2017.v0.a2760

Jessica Davis. (2023, December 28). *Aircraft Stability: 3 Types of Static + Dynamic Aircraft Stability*. Pilotmall.Com. https://www.pilotmall.com/blogs/news/aircraft-stability-3-types-of-static-dynamic-aircraft-stability

Kasnakoğlu, C. (2016). Investigation of multi-input multi-output robust control methods to handle parametric uncertainties in autopilot design. *PLoS ONE*, *11*(10). https://doi.org/10.1371/journal.pone.0165017

Marek M. Cel. (2019). *Cessna 172 Flight Simulation Data*. https://doi.org/10.13140/RG.2.2.27040.51205

National Transportation Safety Board. (1987). *Aviation Investigation Final Report - Accident Number: FTW87LA145*.

National Transportation Safety Board. (2005). *Aviation Investigation Final Report - Accident Number: CHI05CA155*.

National Transportation Safety Board. (2020). *Aviation Investigation Final Report - Accident Number: ERA20CA102*.

Nelson, R. C. (1998). Flight stability and automatic control / Robert C. Nelson. In *Flight stability and automatic control*.

Niall McCarthy. (2021, January 15). *The Most Produced Aircraft Of All-Time* . Www.Statistia. Com. https://www.statista.com/chart/20788/aircraft-models-with-the-highest-estimated-production-figures/

Prach, A. (2022). SDC-based dynamic inversion controller for a fixed-wing aircraft. *MECHANICS OF GYROSCOPIC SYSTEMS*, *43*. https://doi.org/10.20535/0203-3771432022275285

Prach, A., Gursoy, G., & Yavrucuk, L. (2019). Nonlinear controller for a fixed-wing aircraft landing. *Proceedings of the American Control Conference*, *2019-July*. https://doi.org/10.23919/acc.2019.8814970

Sadraey, M. (2020). Automatic Flight Control Systems. *Synthesis Lectures on Mechanical Engineering*, *4*(1). https://doi.org/10.2200/s00968ed1v01y201911mec023

Vadivelu, P., Lakshmanan, D., Naveen, R., Mathivannan, K., & Yoges Kumar, G. (2020). Numerical study on Longitudinal control of Cessna 172 Skyhawk aircraft by Tail arm length. *IOP Conference Series: Materials Science and Engineering*, *764*(1). https://doi.org/10.1088/1757-899X/764/1/012026